Journal of Computer-Aided Molecular Design **18:** 287–302, 2004.

Docking and scoring of metallo-β-lactamases inhibitors

Lars Olsen[a,b], Ingrid Pettersson[c], Lars Hemmingsen[d], Hans-Werner Adolph[e] & Flemming Steen Jørgensen[a,*]

[a]*Department of Medicinal Chemistry, The Danish University of Pharmaceutical Sciences, Universitetsparken 2, DK-2100 Copenhagen, Denmark*

[b]*Department of Mathematics and Physics, The Royal Veterinary and Agricultural University, DK-1871 Frederiksberg C, Denmark*

[c]*Protein Structure, Novo Nordisk A/S, Novo Nordisk Park, DK-2760 Måløv, Denmark*

[d]*Department of Physics, The Quantum Protein Centre, The Technical University of Denmark, DK-2800 Kgs. Lyngby, Denmark*

[e]*Center for Bioinformatics, University of the Saarland and Max-Planck-Institut for Informatics, D-66041 Saarbrücken, Germany*

Received 9 July 2003; accepted in revised form 6 July 2004

Key words: binding, docking, inhibitors, metallo-β-lactamase, scoring function

Summary

The performance of the AutoDock, GOLD and FlexX docking programs was evaluated for docking of dicarboxylic acid inhibitors into metallo-β-lactamases (MBLs). GOLD provided the best overall performance, with RMSDs between experimental and docked structures of 1.8–2.6 Å and a good correlation between the experimentally determined MBL-inhibitor affinities and the GOLD scores. GOLD was selected for a test including a broad spectrum of inhibitors for which experimental MBL-inhibitor binding affinities are available. This study revealed that (1) for most compound classes (dicarboxylic acids, tetrazoles, sulfonylhydrazones, and peptide-like compounds) there is a good correlation between the experimentally determined MBL-inhibitor affinities and the GOLD scores, (2) the correlation only holds within a given class, that is, scores of compounds from different classes cannot be directly compared, (3) for some compound classes (e.g. small sulphur compounds) there is no direct correlation between the experimentally determined MBL-inhibitor affinities and the GOLD scores. Using partial least squares methods, a model with $R^2 = 0.82$ and $Q^2 = 0.78$ for the training set was obtained based on the GOLD score and descriptors associated with binding of the IMP-1 inhibitors to the enzyme. The external Q^2 for the test set is 0.73. This final model for prediction of IMP-1 MBL-inhibitor affinity handled all known classes of MBL-inhibitors, except small sulphur compounds.

Introduction

Emergence of bacterial and viral resistance to drugs is widely accepted to be one of the most serious threats to public health today [1, 2]. Prominent examples are bacterial resistance to penicillin and similar (β-lactam) antibiotics and HIV resistance to anti-HIV drugs. The origin of the problem is that applying a drug provides a selective evolutionary pressure towards emergence of mutants, which are resistant to the drug. The production of β-lactam hydrolysing enzymes, β-lactamases, is the most significant defence mechanism developed by bacteria, to protect them against β-lactam antibiotics. The β-lactamases have been divided into four classes, A–D, based on the amino acid sequences [3]. The class B β-lactamases, the metallo-β-lactamases (MBL), require zinc or other metal ions to function, and pose a particularly potent threat, because several of this class of enzymes hydrolyse a broad spectrum of β-lactam antibiotics, they have spread to pathogenic

*To whom correspondence should be addressed. E-mail: fsj@dfuni.dk

bacteria, and no inhibitors are clinically available at the present time [4, 5]. The class B β-lactamases have been subdivided into three classes, B1–3, depending on their amino acid sequences [6].

A number of structures of class B β-lactamases have been determined by X-ray diffraction for IMP-1 from *Pseudomonas aeruginosa* [7, 8], CcrA from *Bacteroides fragillis* [9–12], BCII from *Bacillus cereus* [13–15] from subclass B1, and L1 from *Stenotrophomonas maltophilia* [16] and Fez-1 from *Legionella gormanii* [17] from subclass B3 showing two metal ion binding sites. In site 1, the metal ion coordinating amino acids are three histidines for most of the enzymes, though some might have one of the histidines replaced with an asparagine based on sequence alignments. In site 2, the metal ion coordinating amino acids are an aspartic acid, a cysteine/histidine, and a histidine for enzymes from subclass B1/B3.

A number of inhibitors have been reported in the literature for the MBLs of subclass B1–B3. These are trifluoromethyl alcohols and ketones [18], biphenyl tetrazoles [12], β-lactams as carbapenem derivatives [19], cephamycins and moxalactam [20], hydroxamic acids [21], thiols [22–25], cysteinyl peptides [24], thioesters [22, 24, 26], mercapto-carboxylates [8, 24, 25, 27], 2,3-disubstituted succinic acids [7], tricyclic natural compounds [28], and sulfonylhydrazones [29]. In particular, the 2,3-disubstituted succinic acids [7] and mercapto-carboxylic inhibitors [8, 24] are potent inhibitors with inhibition constants in the 3–90 nM range.

Some of the crystal structures contain inhibitors. This is the case for IMP-1 for two succinic acids (PDB codes: 1JJT/1JJE) [7], and a mercapto-carboxylic acid compound (PDB code: 1DD6) [8]. For the succinic acids, the carboxylic acids coordinate to the zinc ions, as well as to Lys161 and Asn167, whereas the hydrophobic substituents interact with the hydrophobic amino acid residues in a flexible flap of the enzyme. Complexes for the CcrA enzyme have also been solved with MES (PDB code: 1A7T) [11], a biphenyl tetrazole (PDB code: 1A8T) [12], and tricyclic carboxylic acid (PDB code: 1KR3) [28]. The two latter studies show that mainly the zinc ion site 2 is involved in the binding of the inhibitor.

The availability of several experimentally determined three-dimensional structures of β-lactamases cocrystallized with various inhibitors provides an excellent basis for using structure-based approaches for the discovery of new inhibitors. In structure-based ligand design information of the structural characteristics of the binding site (shape, hydrogen bond donors/acceptors and hydrophobic regions) is used to design ligands with complementary properties. Several examples on structure-based design of new ligands, especially enzyme inhibitors, have been reported [30]. The development of the HIV-1 protease inhibitors provides some of the most convincing and by now classical examples [31].

A variety of computational methods are applied in structure-based ligand design, but central to this process are methods which are able to predict the correct binding mode of a ligand to its macromolecular target protein (docking) [32] as well as methods which are able to predict reliable values for the binding affinity between the ligand and the target (scoring) [33]. The quality of methods for docking small molecules into a target protein has improved considerably in the last two decades. Presently, the best docking methods consider a ligand as fully flexible and evaluate different binding modes as well as different conformations of the ligand. Only a limited number of docking programs allow the flexibility of the target to be taken into account during the docking process, although protein flexibility is generally accepted to be crucial in certain cases [34]. Recent developments include programs which take the orientation of hydrogen binding donors at the target [35] and protein side chain conformers [36] into account, but a complete relaxation of the protein binding site during the docking process is still not feasible due to computational demands.

The binding affinity or scoring is normally calculated based on an energy-based approach using force field-like terms, a statistically derived potential of mean force field or a scoring function involving terms reflecting various types of intermolecular interactions, and numerous examples on scoring functions exist [33]. Improvements of known scoring functions have been achieved by subsequently applying different scoring functions (rescoring) [37] and by applying several scoring functions (consensus scoring) [38, 39]. Furthermore, the choice of scoring function also depends on the problem to be studied, because some scoring functions have been optimised with respect to speed in order to be used for virtual screening [40], whereas others have been developed for giving more reliable estimates of the binding affinity as required in a later stage of the drug discovery process [41].

One possible strategy to overcome the resistance against β-lactam antibiotics is to develop inhibitors for the class B β-lactamases, as has been done for the class A, C, and D β-lactamases. Although docking and scor-

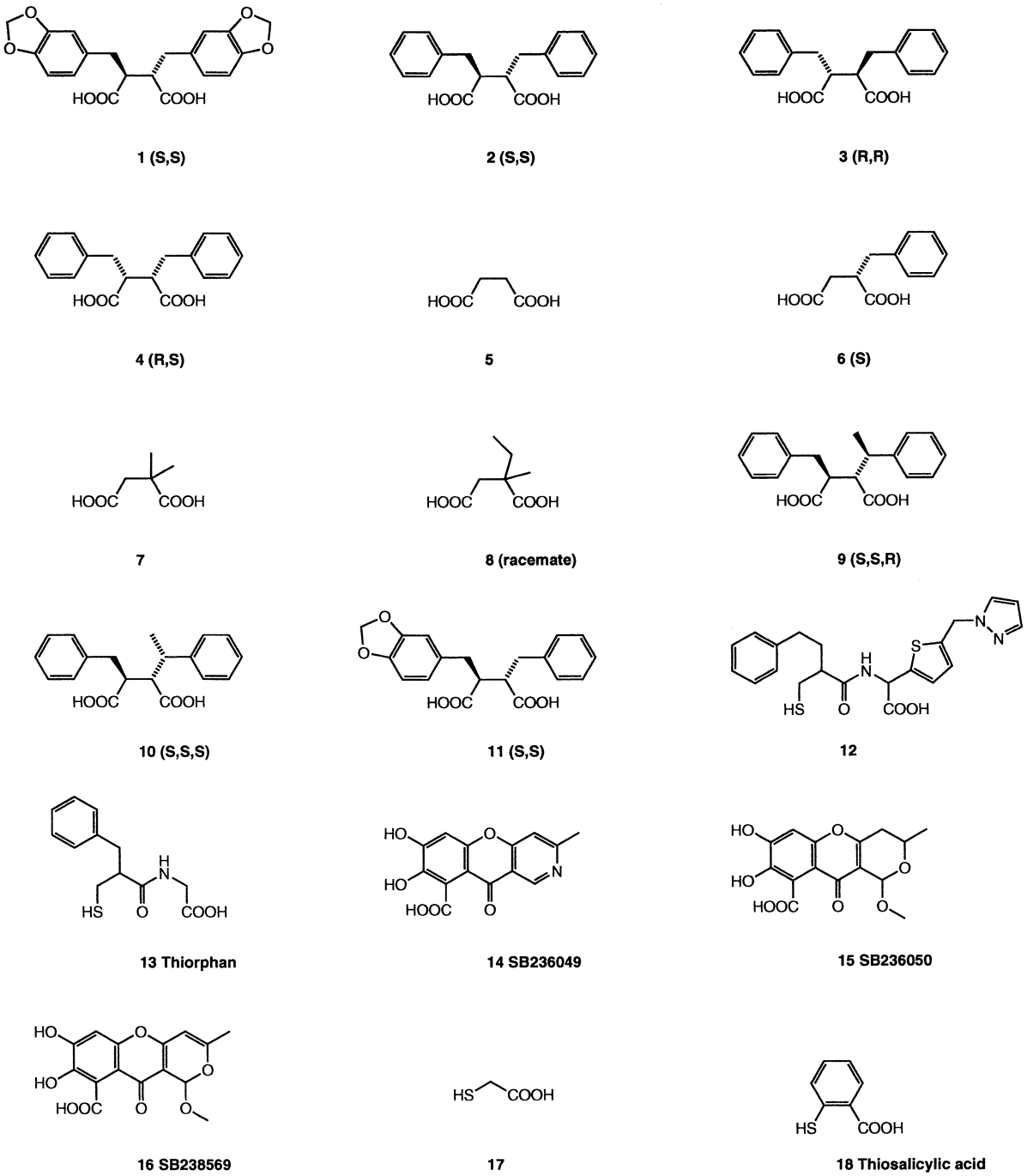

Figure 1. MBL inhibitors. All inhibitors are shown as the neutral species. The docking studies were performed on the form present at neutral pH, except for the thiols (cf. Methods section).

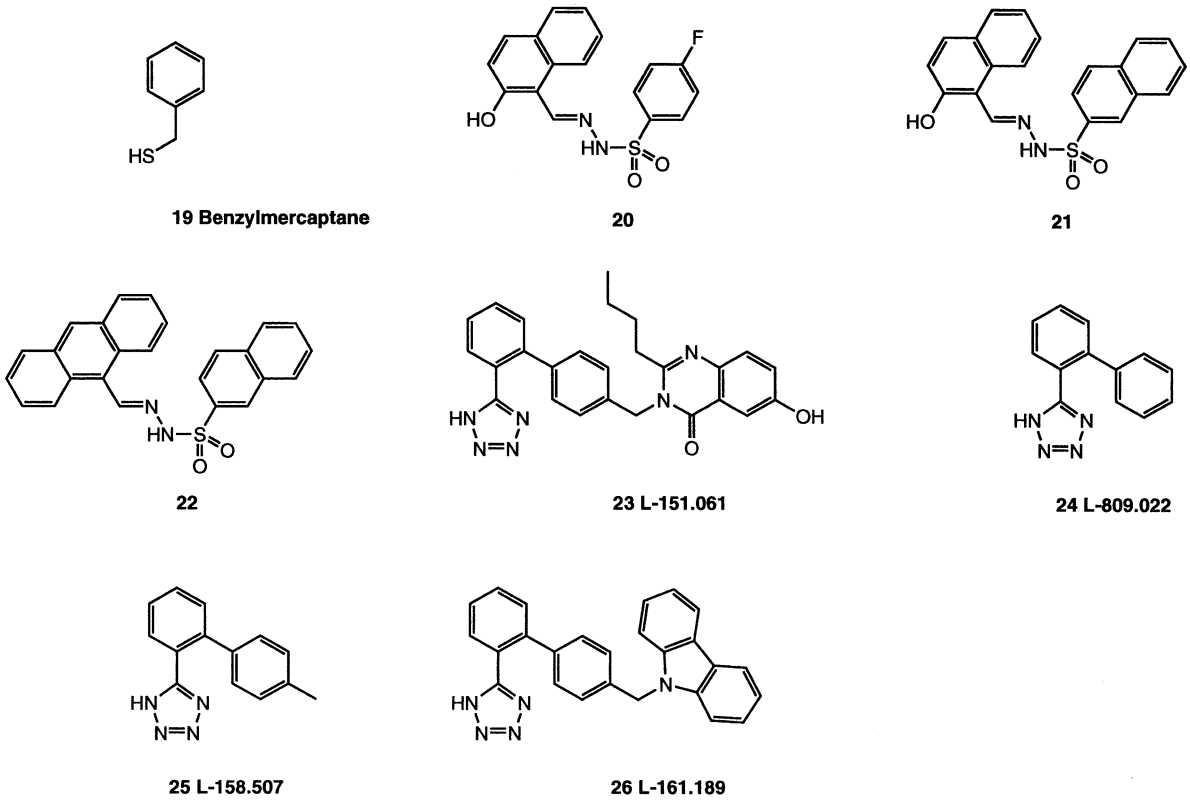

Figure 1. Continued.

ing methods have been intensively evaluated against different structural classes, no studies aimed specifically at their performance against metallo-β-lactamases have been reported. For this particular reason, it is crucial to know which methods are reliable for studying protein-ligand interactions for this class of complexes. In this paper we aim at studying if it is (1) useful to apply some of the most widely used docking programs (AutoDock, FlexX, and GOLD) for these investigations and (2) possible to improve the scoring function used in the dockings.

Methods

Ligands and proteins

Different

Different types of metallo-β-lactamase inhibitors have been reported in the literature. In this study, we focus on the dicarboxylic acids (ligands **1**–**11**), tricyclic natural products (ligands **14**–**16**), peptide-like compounds (ligands **12** and **13**), small sulphur compounds (ligands **17**–**19**), sulphonylhydrazones (ligands **20**–**22**), and biphenyl-tetrazoles (ligands **23**–**26**), cf. Figure 1 and Table 1. These ligands are inhibitors of the IMP-1, CcrA, BCII, and L1 β-lactamases. For the peptide-, sulfonylhydrazone-, and the biphenyltetrazole-series, many very similar inhibitors were reported. Here, we have selected some that represent the range of observed inhibition constants.

Inhibitors, such as hydroxamates, cephamycins and moxalactam [20] have been reported for the MBL from *Aeromonas hydrophila*, but as the three-dimensional structure of the enzyme has not yet been determined, they will not be considered in this work. Other inhibitors are not considered in this work either because the inhibitor may be chemically modified by the enzyme or because it is covalently bound to the enzyme. For example, for the trifluoromethyl ketones, it has been suggested that the ketones may bind to the zinc ions in a hydrated form [18], whereas some thioesters bind irreversibly to the enzyme [26].

Sybyl [42] (version 6.8) was used to build and geometry optimize the ligands. The energy minimizations were carried out with the MMFF force field [43–49]. The ligands were protonated according to the usual

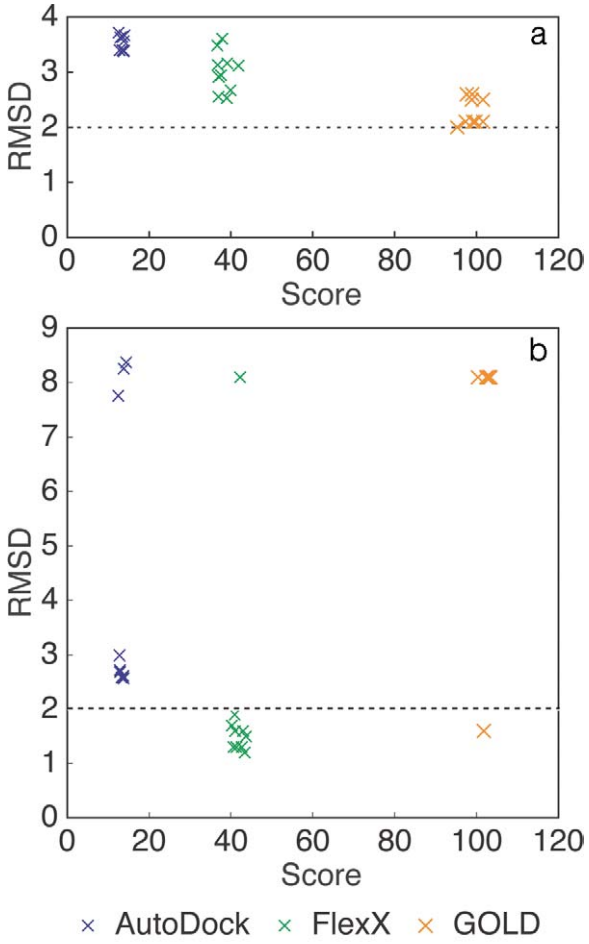

Figure 2. Top: Comparison of scores and RMSDs for ligand **1** docked into IMP-1 (1JJT) by AutoDock, FlexX, and GOLD; bottom: Comparison of scores and RMSDs for ligand **11** docked into IMP-1 (1JJE) by AutoDock, FlexX, and GOLD. The RMSDs (Å) are determined with respect to the crystal structure (1JJT and 1JJE, respectively). The scores obtained with the different programs are not directly comparable.

choice at neutral pH, except for the thiols, that were deprotonated, following experimental evidence for the enzyme-ligand complex [8, 50]. In addition, the sulfonylhydrazones were docked with the sulfone-amide nitrogen either protonated or deprotonated. All ligands are shown in Figure 1.

PDB codes of the proteins used in this work are: 1JJT, 1JJE [7], 1DD6 [8], 1BVT [14], 1A7T [11], 1A8T [12], 1KR3 [28], 1SML [16]. Expect in one case, all water molecules and, if present, ligands were removed from the proteins. Ligand **15**, however, binds to 1KR3 without displacing the water molecule that bridges the two zinc ions. Therefore, it was assumed that the bridging water molecule should be present, when docking ligands **14**–**16**. The crystal structures, which do not contain the bridging water molecule,

Table 1. MBL inhibitors.

Ligand	IC_{50} (μM)	Ref.	Compound class
IMP-1			
1	0.009[a]	7	Dicarboxylic acid
2	0.0027	7	Dicarboxylic acid
3	≥ 0.21	7	Dicarboxylic acid
4	200	7	Dicarboxylic acid
5	6300	7	Dicarboxylic acid
6	490	7	Dicarboxylic acid
7	>10000	7	Dicarboxylic acid
8	>10000	7	Dicarboxylic acid
9	0.013	7	Dicarboxylic acid
10	≥ 2.7	7	Dicarboxylic acid
11	0.0037[b]	7	Dicarboxylic acid
12	0.09[c]	8	Peptide
13	37	28	Peptide
14	151	28	Tricyclic natural product
15	113	28	Tricyclic natural product
16	26	28	Tricyclic natural product
17	1.3	25	Small S-compound
18	200	25	Small S-compound
19	5	25	Small S-compound
20	150	29	Sulfonylhydrazone
21	10	29	Sulfonylhydrazone
22	1.6	29	Sulfonylhydrazone
BCII			
13	5	28	Peptide
14	0.7	28	Tricyclic natural product
15	256	28	Tricyclic natural product
16	19	28	Tricyclic natural product
CcrA			
13	60	28	Peptide
14	2	28	Tricyclic natural product
15	29	28	Tricyclic natural product
16	7	28	Tricyclic natural product
23	1.9[d]	12	Biphenyl-tetrazole
24	860	12	Biphenyl-tetrazole
25	160	12	Biphenyl-tetrazole
26	0.3	12	Biphenyl-tetrazole
L1			
13	5	28	Peptide
14	>1000	28	Tricyclic natural product
15	>1000	28	Tricyclic natural product
16	>1000	28	Tricyclic natural product

[a]PDB: 1JJT, [b]1JJE, [c]1DD6, [d]1A8T.

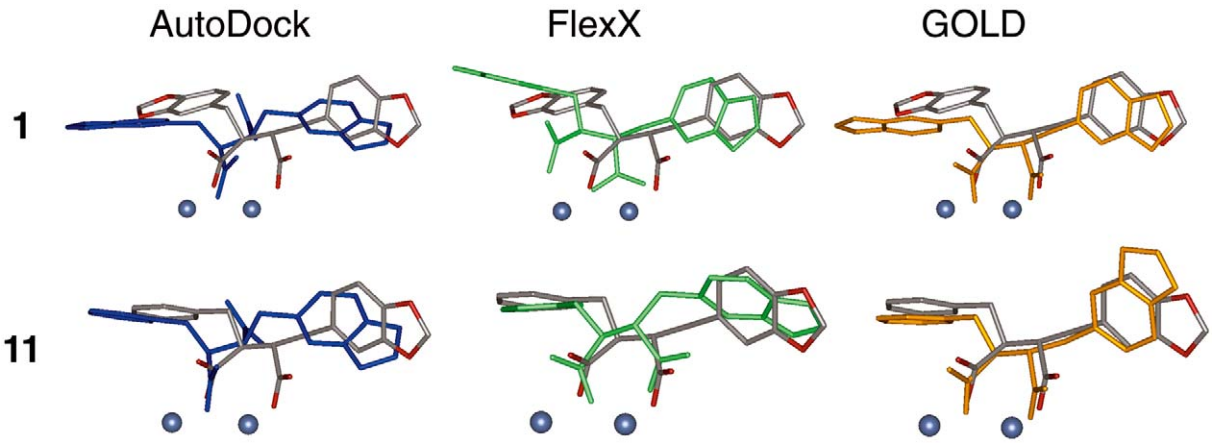

Figure 3. Comparison of the experimentally determined conformation of ligand **1** (top) and **11** (bottom) and the best AudoDock (left), FlexX (middle) and GOLD (right) docked conformations, respectively.

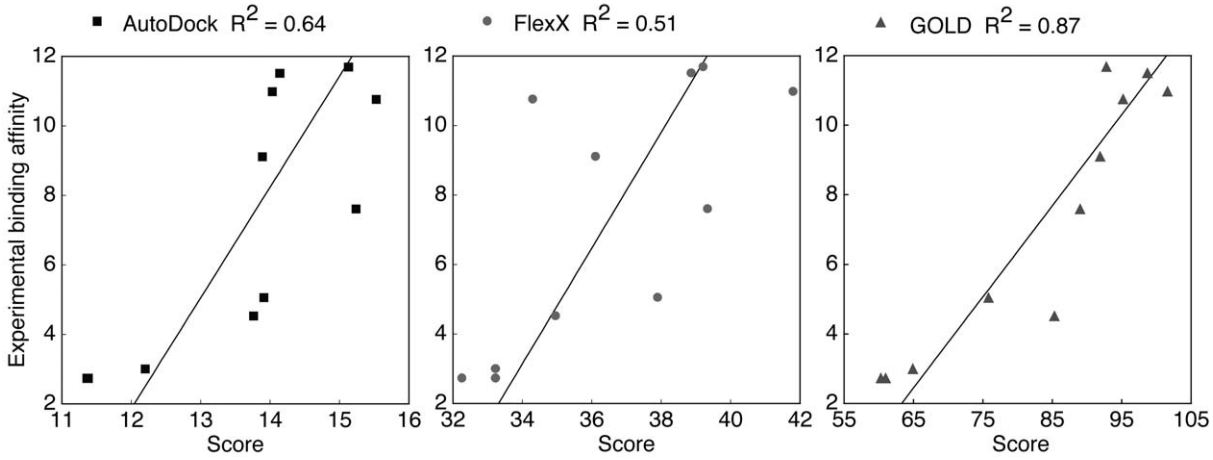

Figure 4. Comparison of scores and experimental binding affinities ($-\log IC_{50}$) for ligands **1**–**11**. The ligands were docked into IMP-1 (1JJT) by AutoDock, FlexX, and Gold. The scores obtained with the different programs are not directly comparable.

were superimposed on 1A7T, and the bridging water molecule was extracted from 1A7T. Hydrogens were added with Sybyl.

Ligands **1**, **11**, **12**, **15** and **23** that have been crystallized with MBL were docked into 1JJT, 1JJE, 1DD6, 1KR3, and 1A8T, respectively. In addition, ligands that belong to the same series as ligands **1**, **15**, and **23** were docked into 1JJT, 1KR3, and 1A8T as well. That is, ligands **1**–**10** were docked into 1JJT, ligand **11** into 1JJE, ligand **12** into 1DD6, ligands **14**–**16** into 1KR3, and ligands **23**–**26** into 1A8T. Other IMP-1, BCII, CcrA, and L1 ligands, for which the three-dimensional structures of MBL-ligand complexes have not been solved, were docked into 1JJT, 1A7T, 1BVT, and 1SML, respectively.

Docking

AutoDock (version 3.0) [51]. The dockings were carried out following the same procedure as described by Hanessian et al. [52]. Amber charges and van der Waals parameters were used for all protein atoms, and for the zinc ions a formal charge of +2 and van der Waals parameters according to Hoops et al. were used [53]. The partial atomic charges of the ligands were determined by using a fit to the electrostatic potential procedure based on the MNDO method [54, 55] as implemented in Sybyl. Each ligand was docked 10 times, and the active site radius selected to be 10 Å from Zn2.

FlexX (version 1.8) [56–59], as implemented in Sybyl. Default settings were used for the dockings.

Each ligand was docked 10 times, and the active site radius selected to 10 Å from Zn2.

GOLD (version 1.2) [35]. Default settings were applied, except that the amide bonds were allowed to flip. Each ligand was docked 10 times, and the active site radius selected to 10 Å from Zn2 for the dockings of ligands **1**–**11**. When docking other types of ligands, an active-site radius of 15 Å was used for the largest ones.

RMSD. All root-mean-square-deviations (RMSDs) were calculated relative to the ligand in the crystal structure only considering non-hydrogen atoms.

Rescoring the complexes

GRID (version 21) [60–63] was used for determination of energy contributions. These contributions to the binding affinity were calculated as described in the GRID manual (section: *Using probe molecules*) [64]. Upon ligand binding, energy is required to displace water molecules pre-bound to the protein (in the following denoted P-H_2O), the ligand (L-H_2O) or the zinc ions (B-H_2O). In addition, ordered water molecules might be displaced from hydrophobic regions of the protein, resulting in the hydrophobic effect (E-hp). For this method, the following directives (keywords) have been recommended to prepare the protein input file (the kout file): DPRO=20.0; FOBE = 1.0; HBND = 1.0; MOVE = 0; TORS = +1.5 kcal/mol; WATA = −4.25 kcal/mol; WENT = −0.848 kcal/mol. The ligand files were prepared with GRID default settings.

Surface areas. The changes in polar and non-polar surface areas (ΔPSA and ΔNPSA, respectively) upon ligand binding were determined using Sybyl. The reported changes in surface areas, ΔA, are calculated using the following equation:

$$\Delta A = A(\text{Protein}) + A(\text{Ligand}) - A(\text{Protein} - \text{Ligand complex})$$

with A = PSA and NPSA, respectively.

Solvation energy of the ligand. The solvation energy (in the following denoted E-solv) of the ligand for its protonation state at neutral pH was determined using the CPCM solvent method [65, 66] at the B3LYP/6-31G(d) level [67–74] for PM3 geometry optimized structures [75–76]. Gaussian98 [77] was used for the calculations with default settings.

Principal Component Analyses (PCA). The Principal Component Analyses were done in Simca-P (version 10.0) [78, 79].

Partial Least Squares (PLS) analyses. The different energy contributions (described above) were fitted to $-\log(IC_{50})$ using the partial least squares (PLS) method implemented in Simca-P (version 10.0) [78, 79]. In the PLS analysis we used the default settings in the Simca-P program with a cross-validation procedure dividing the data into seven groups.

Binding affinities in the PLS models. Only IC_{50} values have been considered in our models, because the number of inhibitors for which K_i values have been determined is considerably smaller. The experimental conditions for determination of the IC_{50} values are comparable (nitrocefin as substrate, excess of zinc ions, and at neutral pH) although from different laboratories [7, 8, 12, 25, 28, 29], except for the substrate concentrations. One should be aware of the fact that an IC_{50} value depends on the substrate concentration. Assuming competitive inhibition, it is possible to obtain an IC_{50} derived inhibition constant. This inhibition constant is determined with the following relation: $K = IC_{50}/(X + 1)$ with $X = [\text{nitrocefin}]/K_m$. Using $-\log(K)$ instead of $-\log(IC_{50})$ in our final PLS model, which includes ligands **1**–**16**, **20**–**22**, resulted in small differences in R^2 (0.01) and Q^2 (0.02). Thus, the models reported in Results and discussion are all based on the original IC_{50} values.

Results and discussion

Succinic acids docked into IMP-1 using AutoDock, FlexX, and GOLD

We have used AutoDock, FlexX, and GOLD to dock a series of succinic acids [7] to evaluate the ability of the programs to reproduce the experimental binding modes and to examine the correlation between the scores and the experimental binding affinities.

Ligand **1** was docked 10 times into IMP-1 (1JJT), using AutoDock, FlexX, and GOLD. The RMSDs with respect to the experimental binding mode are 3.4–3.7 Å, 2.5–3.5 Å, and 2.0–2.6 Å for AutoDock, FlexX, and GOLD, respectively (see Figure 2a). For all three programs the binding modes of the 10 docked structures are found in a narrow range of RMSDs. Generally, the RMSDs seem large (> 2.0 Å), but this is a consequence of the two hydrophobic groups binding in a hydrophobic region of the protein. Considering only the succinic acid-part of the ligand, the RMSDs are 3.0–3.7 Å, 1.1–2.4 Å, and 0.6–0.8 Å for AutoDock, FlexX, and GOLD, respectively.

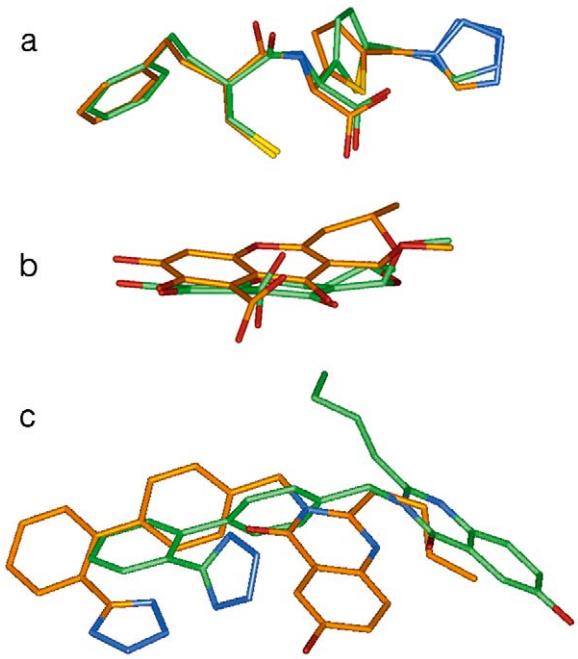

Figure 5. Comparison of docked and experimentally determined conformations. The carbon atoms of the docked conformations are coloured orange and the carbon atoms of the experimentally determined conformations are coloured green. (a) The second highest scoring conformation of ligand **12** docked into IMP-1 (1DD6) compared with the experimentally determined conformation of the ligand. (b) The highest scoring conformation of ligand **15** docked into CcrA (1KR3) compared with the experimentally determined conformation of the ligand. (c) The highest scoring conformation of ligand **23** docked into CcrA (1A8T) compared with the experimentally determined conformation of the ligand.

Ligand **11** was docked into IMP-1 (1JJE) 10 times as well. In general, both small (1–3 Å) and large (∼8 Å) RMSDs with respect to the experimental binding modes are observed (see Figure 2b). The large RMSDs correspond to ligands with the aryl-group instead of the phenyl-group placed in the hydrophobic groove. Autodock and FlexX have most poses in the low RMSD region (RMSD = 2.6–2.7 Å and 1.2–1.9 Å, respectively), whereas GOLD only finds one structure with low RMSD (1.6 Å). However, FlexX and GOLD reproduce the metal binding well with RMSDs of 0.7–0.9 Å and 0.5–0.6 Å, respectively, for the succinic acid-part of the ligand.

In Figure 3 we have compared the best docked conformations of ligands **1** and **11** with the conformations found experimentally in the enzyme-ligand complexes. For both **1** and **11** AutoDock predicts a binding mode with only one carboxylate group coordinating to the zinc ions. Accordingly, the conformations found by AutoDock differ considerably from the conformations found experimentally. FlexX predicts for both **1** and **11** that both carboxylate groups coordinate to the zinc ions, but for **1** it is the wrong carboxylate group which has contact to both zinc ions, leading to a poor prediction for this compound. GOLD predicts for both

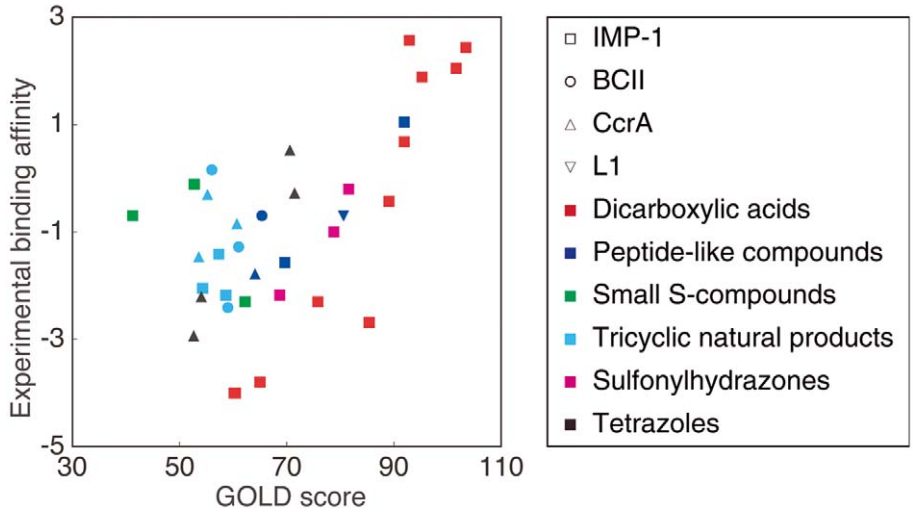

Figure 6. Plot of experimental binding affinities (−log IC_{50}, cf. Table 1) *versus* GOLD scores. Dicarboxylic acids: Ligands **1**–**11** (IMP-1); Tricyclic natural products: Ligands **14**–**16** (IMP-1, CcrA, BCII, L1); Peptide-like compounds: Ligands **12, 13** (IMP-1); Small sulphur compounds: Ligands **17** (IMP-1), **18, 19** (IMP-1, BCII); Biphenyl-tetrazoles: Ligands **23**–**26** (CcrA); Sulfonylhydrazones: Ligands **20**–**22** (IMP-1).

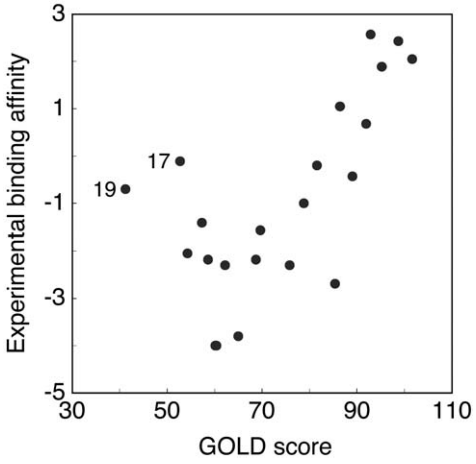

Figure 7. Plot of experimental binding affinities ($-\log IC_{50}$) *versus* GOLD scores for ligands **1**–**22** ($R^2 = 0.45$). The small sulphur compounds **17** and **19** are labelled.

1 and **11** conformations very similar to the conformations found experimentally. It is also interesting to notice that the structures with correct binding to the zinc ions also place the hydrophobic groups correctly (**11** by FlexX and both **1** and **11** by GOLD), probably reflecting that the charge-charge interactions dominate over hydrophobic interactions.

In order to test the performance of the scoring functions in AutoDock, FlexX, and GOLD, ligands **1**–**11** were all docked into IMP-1 (1JJT). Figure 4 shows the best score from each docking, plotted against the experimental binding affinity. Correlation between the scores and experimental binding affinities is obtained by all three programs. The correlation obtained by GOLD ($R^2 = 0.87$) is considerably better than those obtained byAutoDock ($R^2 = 0.64$) and FlexX ($R^2 = 0.51$).

In summary, the GOLD program provides the largest number of docked conformations with low RMSD with respect to the crystal structure for ligand **1** docked into IMP-1 (cf. Figure 2a). Docking ligand **11** into IMP-1, FlexX and GOLD give the largest number of docked conformations with low RMSD (cf. Figure 2b). Finally, the best correlation between score and experimentally determined binding affinity is found for GOLD (cf. Figure 4). Thus, we chose to use GOLD in the subsequent analysis of ligand binding to the MBLs.

Evaluation of the binding modes of other types of MBL inhibitors using GOLD

The evaluation of the three docking programs shows that GOLD seems to be well suited for docking ligands into MBLs, at least for the succinic acid series. As already mentioned, other types of MBL inhibitors than the succinic acids have been reported in the literature. These include tricyclic natural products, peptide-like and small sulphur compounds, biphenyl-tetrazoles, and sulphonyl hydrazones. Ligands **12**, **15**, and **23** are examples of the peptide-like compounds, tricyclic natural products, and the biphenyl-tetrazoles, respectively, for which the three-dimensional structure of the MBL-inhibitor complex has been determined by X-ray crystallography.

*Ligand **12** docked into IMP-1 (1DD6).* Docking ligand **12** into 1DD6 10 times results in structures, for which the RMSDs generally are 2–3 Å. However, the second highest scoring structure has a binding mode that is in excellent agreement with the experimental structure (RMSD = 0.5 Å) (cf. Figure 5a).

*Ligand **15** (SB236050) docked into CcrA (1KR3).* Ligand **15** was docked into the protein containing the bridging water molecule, as in the experimental structure. The RMSDs range from 0.6–6.3 Å. The five highest scoring structures have RMSDs smaller than 1 Å with respect to the experimental structure (cf. Figure 5b).

*Ligand **23** (L-151061) docked into CcrA (1A8T).* For ligand **23**, the RMSDs are in the range of 4–5 Å as compared to the crystal structure. This ligand appears to be a difficult case for the GOLD program. However, the ligand is a relatively large molecule, and it is particularly the part of the molecule that is not coordinating the Zn ion, that differs from the experimental structure (cf. Figure 5c). The RMSDs for the biphenyl-tetrazole part of the ligands are around 3 Å for ligand **23**. It is noteworthy that for the three other biphenyl-tetrazole ligands **24**–**26**, GOLD places the biphenyl-tetrazole part of these ligands similar to the biphenyl-tetrazole part of **23** in the X-ray structure (RMSD = 1–2 Å).

Thus, the docked structures of ligands **12** and **15** are in excellent agreement with the experimental binding modes, as was the case for the succinic acids, whereas ligand **23** seems to be a harder case for the GOLD program.

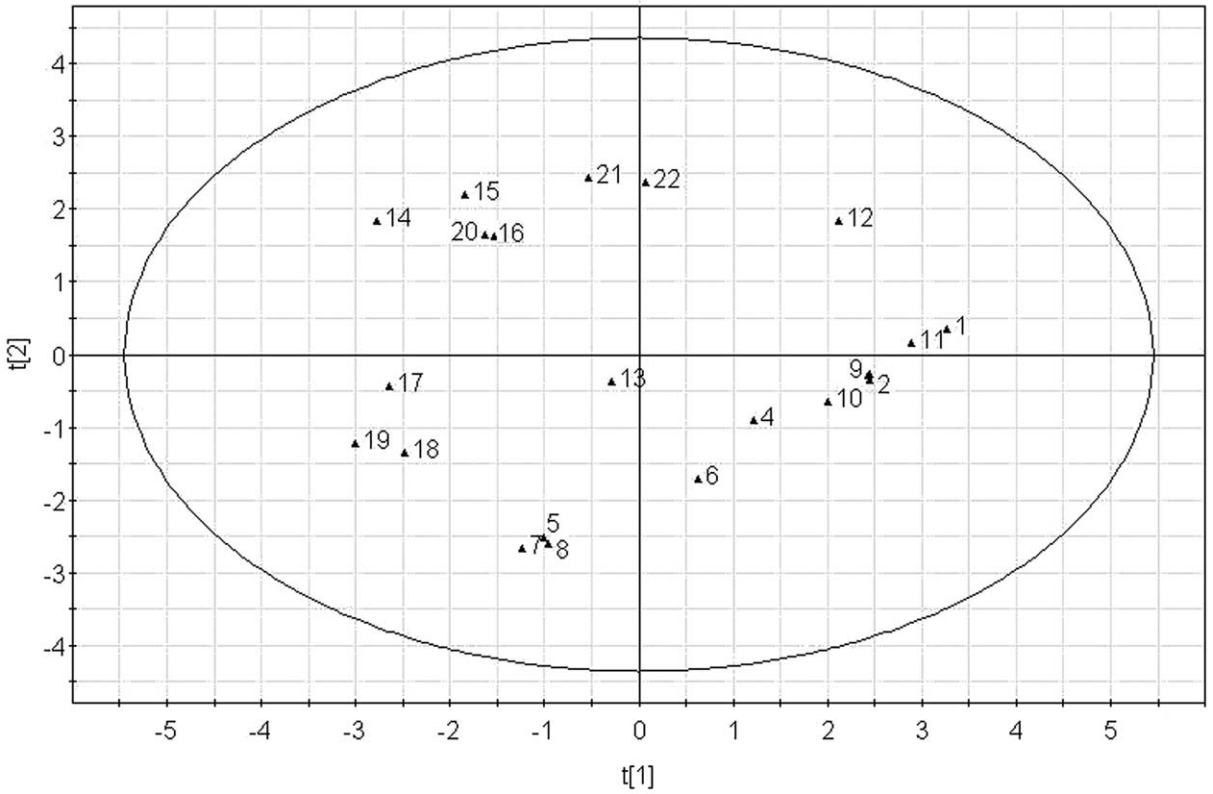

Figure 8. PCA scores plot for ligands **1**–**22**. The GOLD score, P-H_2O, L-H_2O, B-H_2O, E-hp, ΔPSA, ΔNPSA, E-solv, and tors are used in the PLS model. The following clusters are observed: dicarboxylic acids with aromatic substituents (ligands **1**–**4**, **6** and **9**–**11**), dicarboxylic acids without aromatic substituents (ligands **5**, **7** and **8**), tricyclic natural products (ligands **14**–**16**), sulfonylhydrazones (ligands **20**–**22**) and the small sulphur compounds (ligands **17**–**19**). The two peptide-like compounds (ligands **12** and **13**) constitute a less well defined cluster.

Comparison of GOLD scores with experimental binding affinities

The remaining MBL inhibitors in Figure 1, for which IC_{50} values have been determined, were docked into IMP-1, CcrA, BCII, and L1. In Figure 6 the experimental binding affinities are plotted versus the GOLD scores. The inhibitors have been divided into six structural classes: dicarboxylic acids, tricyclic natural compounds, peptide-like compounds, small sulphur compounds, biphenyl-tetrazoles, and sulfonylhydrazones. Comparing the different series, it can be seen that the GOLD score is shifted vertically for the different series. It is possible to correlate the experimental binding affinities and the GOLD scores for the dicarboxylic acids, the peptide-like compounds, and the biphenyl-tetrazole inhibitors, respectively.

For the sulfonylhydrazone compounds (ligands **20**–**22**), a correlation between the GOLD scores and the experimental binding affinities is observed as well. The GOLD scores in Figure 6 correspond to sulfonylhydrazones docked with neutral sulphone-amide nitrogens. However, the pK_a of the sulphone-amide hydrogen may be low enough (8.5 [80]) for the nitrogen to be deprotonated, when bound to the active site of the β-lactamases. Therefore, we also docked ligands **20**–**22** into IMP-1 in their deprotonated forms. The corresponding GOLD scores were 74, 81 and 82 for ligands **20**–**22**, respectively, and a slightly different binding mode (now with the deprotonated sulphone-amide nitrogen close to Zn2) was obtained. Overall the scores and conformations are similar for the neutral and deprotonated forms of these ligands. The correlations presented in the following sections do not depend on the protonation state of the sulfonylhydrazones.

The light blue points (cf. Figure 6) correspond to three different tricyclic natural product compounds (ligands **14**–**16**) bound to IMP-1, CcrA, and BCII. For these compounds there is no correlation between the GOLD score and the experimentally determined binding affinity, and they have very low GOLD scores, as compared to e.g. the dicarboxylic acids and peptide-like compounds. The latter might be caused by the

fact that these ligands have been docked into a protein containing the bridging water molecule, in accordance with the experimental structure. That is, energy is not required to remove the structural bridging water molecule for this type of ligands, as for all other types of ligands considered in this work. In practice, this is an effect that is difficult to take into account in the comparison with other compound classes, but it is definitely important for the binding of the inhibitor.

Only a weak correlation is observed for the small sulphur-containing compounds (cf. Figure 6), i.e. ligands **17**–**19**. It is interesting that these compounds have such low GOLD scores. One might speculate that this is due to the sulphur parameters in the GOLD scoring function. However, most of the peptides also contain a free thiol-group, and they have much higher scores, suggesting that this is not the problem. Another common feature for the small sulphur-containing compounds is that they have only a few torsional degrees of freedom. That is, they do not lose much entropy upon ligand binding, as compared to most of the other compounds in the data set. Furthermore, these compounds are smaller than the others, and a change in the active site cannot be ruled out. The distance between the metal binding group and the phenyl ring of ligand **18** is shorter than the corresponding distance for e.g. ligands **12** and **13**, and the distance to the hydrophobic amino acid residues in the flexible loop might be too long to interact with the non-polar parts of the small sulphur ligands. It has been observed experimentally that the flexible loop closes on the substrate binding site upon binding of ligands [6]. In this work we have not included the energy associated with a conformational change of the protein and/or the change in hydrophobic interactions resulting from such a change. If this energy contribution is responsible for the systematic deviations of the score of the small sulphur ligands from the other ligands, it would be necessary to include protein flexibility in the docking [36].

In conclusion, Figure 6 shows that it is not possible to obtain one correlation for all MBL inhibitors covering all the bacterial targets studied in this work, i.e. the IMP-1, CcrA, L1, and BCII lactamases. Figure 6 also indicates that a correlation between the GOLD scores and the experimental binding affinities is obtained for different series of compounds. This is important in the process of identifying potential drug candidates, when working on series of similar compounds. In the following we will describe the development of predictive models for inhibitors against one of the bacterial enzymes, the IMP-1 lactamase.

Model for scoring of IMP-1 ligands

Considering only those inhibitors tested against IMP-1, i.e. ligands **1**–**22**, and using the GOLD score, binding affinities could be predicted. In Figure 7 the GOLD scores are plotted against the experimental binding affinities, but the correlation coefficient, $R^2 = 0.45$, for this model is not impressive. For two of the compounds, **17** and **19**, the binding affinity is considerably underestimated. Compounds **17** and **19** together with compound **18** are all small sulphur compounds, which do not contain the two hydrophobic groups present in most of the other inhibitors.

As previously pointed out, the small sulphur compounds were also scattered considerably more than the inhibitors in the other structural classes (cf. Figure 6). Thus, it may be concluded that these compounds cannot be handled properly with the present scoring functions simultaneously with the other structural classes of MBL inhibitors. The possibility of developing a model only for this structural class of inhibitors has not been attempted due to the limited number of inhibitors.

By excluding the small sulphur compounds, i.e. ligands **17**–**19**, the correlation coefficient for the IMP-1 inhibitors increases to $R^2 = 0.69$, which must be characterized as a reasonable value considering the structural diversity of the inhibitors.

Rescoring of the IMP-1-ligand complexes

The GOLD score accounts for inter- and intramolecular van der Waals interactions, hydrogen bonding contributions, as well as the torsional energy of the ligand. In order to improve the prediction of binding affinities for the MBL inhibitors we have included a number of additional descriptors representing various effects associated with the recognition or binding process. These additional terms include the energies associated with removal of water molecules pre-bound to the protein and the ligand (P-H_2O and L-H_2O, respectively), possible water bridges between the protein and the ligand (B-H_2O), and the hydrophobic effect (E-hp), the change in polar and non-polar surface areas (ΔPSA and ΔNPSA, respectively), and an estimate of the loss of entropy upon ligand binding that was approximated by the number of rotatable bonds (tors). Some of these descriptors, E-hp and ΔNPSA, may to some extent already be implicitly included in the GOLD score. The numerical values of the energy variables that were included in the models are given in Table 2.

A Principal Component Analysis (PCA) of the GOLD score and the above-mentioned descriptors for

Table 2. Descriptors (X-variables) and experimental binding affinities (Y-variable) used for the PC and PLS analyses. P-H_2O: Penalty for displacing pre-bound water molecules from the protein (kcal/mol); L-H_2O: Penalty for displacing pre-bound water molecules from the ligand (kcal/mol); B-H_2O: Penalty for displacing water molecules bridging the zinc ions (kcal/mol); E-hp: Hydrophobic energy (kcal/mol); ΔPSA: Change of polar surface area upon ligand binding (Å^2); ΔNPSA: Change of non-polar surface area upon ligand binding (Å^2); E-solv: Solvation energy of the ligand at neutral pH (kcal/mol); tors: Number of rotatable bonds.

Ligand	GOLD score	P-H_2O	L-H_2O	B-H_2O	E-hp	ΔPSA	ΔNPSA	E-solv	tors	−log(IC50)
Training set										
1	101.62	16.13	19.14	8.25	6.79	239.12	710.18	187.25	7	2.05
4	75.81	15.61	15.53	8.25	6.79	165.31	623.67	180.81	7	−2.30
5	64.99	13.69	11.86	8.25	–	184.40	295.45	212.42	3	−3.80
6	85.38	14.05	16.48	8.25	5.09	171.33	462.78	194.30	5	−2.69
7	60.39	14.11	12.21	8.25	3.39	163.81	360.15	205.37	3	−4.00
8	60.15	13.84	13.01	8.25	3.39	155.36	404.65	202.68	4	−4.00
9	95.22	16.06	15.11	8.25	6.79	167.69	644.20	176.03	7	1.89
10	89.05	16.18	16.69	8.25	6.79	160.74	644.83	172.01	7	−0.43
11	98.71	15.89	16.77	8.25	6.79	209.39	670.21	181.18	7	2.43
13	69.63	11.23	12.23	8.29	5.09	179.57	529.97	56.57	6	−1.57
15	54.29	3.62	15.50	0.00	6.79	257.13	624.27	60.87	2	−2.05
16	57.32	4.76	16.25	2.48	6.79	244.15	569.56	59.41	2	−1.41
21	78.80	2.67	9.52	8.29	10.18	190.33	689.16	11.85	4	−1.00
Test set										
2	92.86	15.76	15.13	8.25	6.79	159.10	627.78	183.76	7	2.57
3	91.92	16.95	17.04	8.25	8.48	164.00	606.65	183.76	7	0.68
12	86.42	13.53	11.20	8.25	6.79	293.63	741.50	54.10	10	1.05
14	58.62	1.56	11.53	0.00	6.79	237.41	485.61	66.16	1	−2.18
20	68.70	1.87	6.08	8.29	8.48	173.47	616.98	12.17	4	−2.18
22	81.56	10.73	5.50	8.29	10.18	195.43	770.05	6.47	4	−0.20
Excluded										
17	52.73	7.72	7.40	6.36	–	176.15	249.92	66.84	1	−0.11
18	62.21	10.30	6.93	8.29	3.39	163.03	344.66	57.07	1	−2.30
19	41.23	8.29	–	8.29	5.09	75.21	337.40	2.85	1	−0.70

the IMP-1 inhibitors yielded a four-component model with $R^2 = 0.94$ and $Q^2 = 0.69$. In the scores plot of the two first components (cf. Figure 8) the ligands are clustered according to their structural class, i.e. dicarboxylic acids with and without aromatic substituents (ligands **1**–**4**, **6** and **9**–**11** in one group and ligands **5**, **7** and **8** in another group, respectively), tricyclic natural products (ligands **14**–**16**), sulfonylhydrazones (ligands **20**–**22**) and the small sulphur compounds (ligands **17**–**19**). The two peptides (ligands **12** and **13**) constitute a less well defined cluster. Although the small sulphur compounds are not outliers in the PCA scores plot, they constitute a well-defined cluster. Thus, the descriptors are apparently able to describe the structural differences between the inhibitors.

An initial model for the binding affinity for the IMP-1 inhibitors was constructed by a Partial Least Squares (PLS) analysis using the previously discussed descriptors as X-variables. The compounds for which IC_{50} values are available were used as observations with $-\log(IC_{50})$ as the Y-variable (cf. Table 2). This initial PLS model had $R^2 = 0.43$ and $Q^2 = 0.30$, which is comparable to the model which only used the GOLD score as descriptor ($R^2 = 0.45$) (cf. Table 3).

The plot of predicted versus experimental binding affinities for the initial PLS model (not shown) was very similar to Figure 7, with a considerable underestimation of the binding affinity for compounds **17** and **19**. Based on this observation it was decided also to exclude the small sulphur compounds from the PLS

Table 3. PLS models for prediction of binding affinity of IMP-1 inhibitors. GOLD score, P-H_2O, L-H_2O, B-H_2O, E-hp, ΔPSA, ΔNPSA, E-solv, and tors were used as variable in the models. P-H_2O: Penalty for displacing pre-bound water molecules from the protein (kcal/mol); L-H_2O: Penalty for displacing pre-bound water molecules from the ligand (kcal/mol); B-H_2O: Penalty for displacing water molecules bridging the zinc ions (kcal/mol); E-hp: Hydrophobic energy (kcal/mol); ΔPSA: Change of polar surface area upon ligand binding (Å^2); ΔNPSA: Change of non-polar surface area upon ligand binding (Å^2); E-solv: Solvation energy of the ligand at neutral pH (kcal/mol); tors: Number of rotatable bonds. A: Ligands **1**–**22** are included in the model. B: Ligands **1**–**16**, **20**–**22** are included in the model.

Ligands	Number of variables	Type of variables	Number of principal components	R^2	Q^2
A	9	GOLD score, P-H_2O, L-H_2O, B-H_2O, E-hp, ΔPSA, ΔNPSA, E-solv, tors	1	0.43	0.30
B	9	GOLD score, P-H_2O, L-H_2O, B-H_2O, E-hp, ΔPSA, ΔNPSA, E-solv, tors	2	0.80	0.73
Training set	9	GOLD score, P-H_2O, L-H_2O, B-H_2O, E-hp, ΔPSA, ΔNPSA, E-solv, tors	1	0.82	0.78
Test set	9	GOLD score, P-H_2O, L-H_2O, B-H_2O, E-hp, ΔPSA, ΔNPSA, E-solv, tors			0.73

analysis. An improved PLS model with $R^2 = 0.80$ and $Q^2 = 0.73$ could be obtained for the remaining 19 compounds using the same set of X-variables (cf. Figure 9).

The compounds were divided into a training set and a test set (cf. Table 2). Both the training set and the test set contained compounds from all structural classes and included both potent and very weak inhibitors. The PLS model for the training set is a one-component model with $R^2 = 0.82$ and $Q^2 = 0.78$ (cf. Table 3). The external Q^2 for the test set is 0.73. The high R^2 and Q^2 in combination with a high Q^2 for the test set shows that this is a predictive model. Several PLS models were generated based on various training and test sets, and if both sets contained compounds from all structural classes the PLS model was extremely robust, yielding nearly identical R^2 and Q^2 values. The observed versus predicted biological activity is shown for both the training set and the test set in Figure 9a. The coefficient plot (Figure 9b) shows that the largest contributions arise from the GOLD score and ΔNPSA descriptor and somewhat smaller contributions from L-HOH, E-hp and tors. All these contribute positively to the experimental binding affinity. Whereas it seems reasonable that both ΔNPSA and E-hp favour binding, it is more surprising that tors contributes positively to the binding affinity. This is probably caused by the fact that the most potent inhibitors in our data set are also the most flexible ones.

The sulfonylhydrazones (ligands **20**–**22**) deserve a comment, because it is, to our knowledge, unknown if they bind to the MBL with the sulphone-amide nitrogen being neutral or deprotonated. Thus, models were constructed resembling both possibilities, but the protonation state did not change the quality of the models significantly and only the data for the neutral sulfonylhydrazones have been reported here.

Finally, it should be mentioned that the exact binding constants of ligands **7** and **8** have not been determined. As mentioned in Table 1, the IC_{50} values are larger than 10000 μM. Even though the exact IC_{50} values have not been determined, it indicates that these compounds are very weak inhibitors, and therefore this information should be included in the model. Although the aim of this work was to improve scoring functions to enable the identification of novel potent inhibitors, it is important that the models are not solely based on potent inhibitors.

Conclusions

We have evaluated three of the most widely applied docking programs, AutoDock, FlexX, and GOLD, specifically focussing on inhibitors binding to MBL. The studies on a series of succinic acid inhibitors of IMP-1 show that for the docking and the scoring, GOLD performs well. Therefore, GOLD was used for the investigations including inhibitors of IMP-1, CcrA, BCII, and L1, that may be divided into the following structural classes: dicarboxylic acids, peptides, small sulphur compounds, tricyclic natural products, sulfonylhydrazones, and biphenyltetrazoles. Correlation

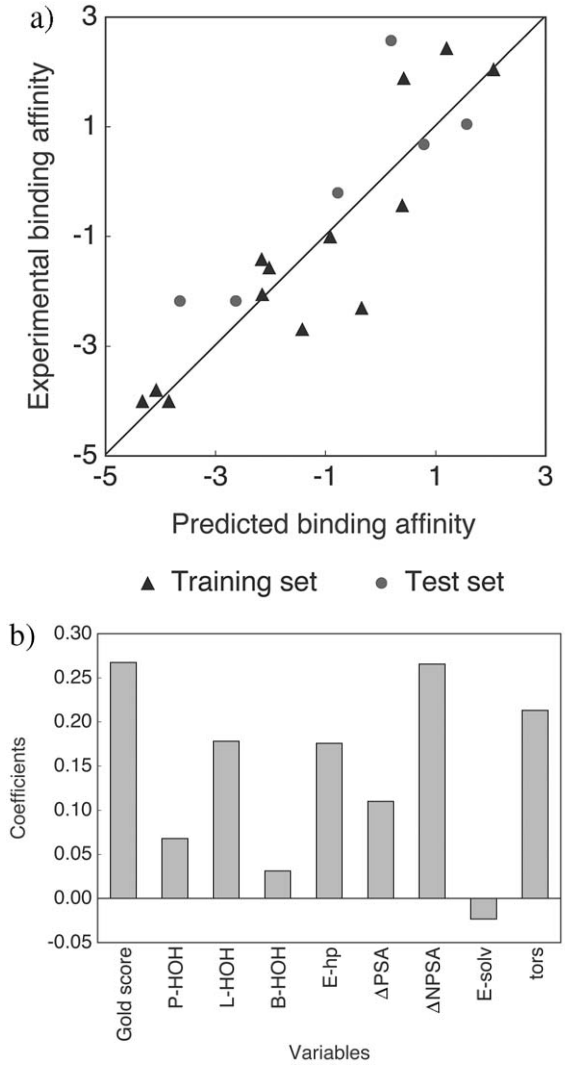

Figure 9. Characteristics for the final PLS model with $R^2 = 0.82$ and $Q^2 = 0.78$ for the ligands **1**–**16**, and **20**–**22**, i.e. excluding the small sulphur compounds. The X-variables are the GOLD score, P-H_2O, L-H_2O, B-H_2O, E-hp, ΔPSA, ΔNPSA, E-solv, and tors. (a) Predicted versus experimental binding affinities ($-\log IC_{50}$). (b) PLS coefficients.

between the GOLD scores and experimental binding affinities was obtained for the dicarboxylic acids, peptides, sulfonylhydrazones, and biphenyltetrazoles, whereas the small sulphur inhibitors showed only a weak correlation, and the tricyclic natural compounds did not show any correlation. It is important that the GOLD score correlates well with the experimental binding affinity within most series of compounds, which means that the GOLD program may be used to identify potent inhibitors.

Several additional contributions to the experimental binding affinity, other than those included in the GOLD score were determined and included in PLS models for the IMP-1 inhibitors. It was not possible to obtain a model that included all IMP-1 inhibitors, but by excluding three small sulphur-containing inhibitors a model with a correlation of $R^2 = 0.82$ and $Q^2 = 0.78$ between predicted and experimental binding affinities was obtained.

Acknowledgements

We are grateful to Novo Nordisk for financial support and to Tripos Associates for the support in connection with our use of Sybyl.

References

1. Medeiros, A.A., Clin. Infect. Diseases, 24 (1997) 19.
2. Matagne, A., Dubus, A., Galleni, M. and Frere, J.-M., Nat. Prod. Rep., 16 (1999) 1.
3. Ambler, R.P., Philos. Trans. R. Soc. London, 289 (1980) 321.
4. Cornaglia, G., Riccio, M.L., Mazzariol, A., Lauretti, L., Fontana, R. and Rossolini, G.M., Lancet, 353 (1999) 899.
5. Livermore, D.M. and Woodford, N., Curr. Opin. Microbiol., 3 (2000) 489.
6. Galleni, M., Lamotte-Brasseur, J., Rossolini, G.M., Spencer, J., Dideberg, O. and Frère, J.-M., Antimicrob. Agents Chemother., 45 (2001) 660.
7. Toney, J.H., Hammond, G.G., Fitzgerald, P.M.D., Sharma, N., Balkovec, J.M., Rouen, G.P., Olson, S.H., Hammond, M.L., Greenlee, M.L. and Gao, Y.-D., J. Biol. Chem., 276 (2001) 31913.
8. Concha, N.O., Janson, C.A., Rowling, P., Pearson, S., Cheever, C.A., Clarke, B.P., Lewis, C., Galleni, M., Frère, J.-M., Payne, D.J., Bateson, J.H. and Abdel-Meguid, S.S., Biochemistry, 39 (2000) 4288.
9. Concha, N.O., Rasmussen, B.A., Bush, K. and Herzberg, O., Structure, 4 (1996) 823.
10. Concha, N.O., Rasmussen, B.A., Bush, K. and Herzberg, O., Protein Sci., 6 (1997) 2671.
11. Fitzgerald, P.M.D., Wu, J.K. and Toney, J.H., Biochemistry, 37 (1998) 6791.
12. Toney, J.H., Fitzgerald, P.M.D., Grover-Sharma. N., Olson, S.H., May, W.J., Sundelof, J.G., Vanderwall, D.E., Cleary, K.A., Grant, S.K., Wu, J.K., Kozarich, J.W., Pompliano, D.L. and Hammond, G.G., Chem. Biol., 5 (1998) 185.
13. Carfi, A., Pares, S., Duée, E., Galleni, M., Duez, C., Frére, J.-F. and Dideberg, O., EMBO J., 14 (1995) 4914.
14. Carfi, A., Duée, E., Paul-Soto, R., Galleni, M., Frère, J.-M. and Dideberg, O. Acta Crystallogr., D54 (1998) 47.
15. Fabiane, S.M., Sohi, M.K., Wan, T., Payne, D.J., Bateson, J.H., Mitchell, T. and Sutton, B.J., Biochemistry, 37 (1998) 12404.
16. Ullah, J.H., Walsh, T.R., Taylor, I.A., Emery, D.C., Verma, C.S., Gamblin, S.J. and Spencer, J., J. Mol. Biol., 284 (1998) 125.

17. Garzía, I., Mercuri, P.S., Papamicael, C., Kahn, R., Frére, J.-M., Galleni, M., Rossolini, G.M. and Dideberg, O., J. Mol. Biol., 325 (2003) 651.
18. Walter, M.W., Felici, A., Galleni, M., Paul-Soto, R., Adlington, R.M., Baldwin, J.E., Frére, J.-M., Gololobov, M. and Schofield, C.J., Bioorg. Med. Chem. Lett., 6 (1996) 2455.
19. Nagano, R., Adachi, Y., Imamura, H., Yamada, K., Hashizume, T. and Morishima, H., Antimicrob. Agents Chemother., 43 (1999) 2497.
20. Zervosen, A., Valladares, M.H., Devreese, B., Prosperi-Meys, C., Adolph, H.-W., Mercuri, P.S., Vanhove, M., Amicosante, G., Beeumen, J.v. and Frère, J.-M., Eur. J. Biochem., 268 (2001) 3840.
21. Walter, M.W., Valladares, M.H., Adllington, R.M., Amicosante, G., Baldwin, J.E., Frère, J.-M., Galleni, M., Rossolini, G.M. and Schoefield, C.J., Bioorg. Chem., 27 (1999) 35.
22. Yang, K.W. and Crowder, M.W., Arch. Biochem. Biophys., 368 (1999) 1.
23. Bounaga, S., Galleni, M., Laws, A.P. and Page, M.I., Bioorg. Med. Chem., 9 (2001) 503.
24. Mollard, C., Moali, C., Papamicael, C., Damblon, C., Vessilier, S., Amicosante, G., Schofield, C.J., Galleni, M., Frère, J.-M. and Roberts, G.C.K., J. Biol. Chem., 276 (2001) 45015.
25. Siemann, S., Clarke, A.J., Viswanatha, T. and Dmitrienko, G.I., Biochemistry, 42 (2003) 1673.
26. Payne, D.J., Bateson, J.H., Gasson, B.C., Proctor, D., Khushi, T., Farmer, T.H., Tolson, D.A., Bell, D., Skett, P.W., Marshall, C., Reid, R., Ghosez, L., Combret, Y. and Marchand-Brynaert, J., Antimicrob. Agents Chemother., 41 (1997) 135.
27. Heinz, U., Wommer, S., Meyer-Klaucke, W., Bauer, R., Papamicael, C., Bateson, J. and Adolph., H.-W., J. Biol. Chem., 278 (2003) 20659.
28. Payne, D.J., Hueso-Rodríguez, J.A., Boyd, H., Concha, N.O., Janson, C.A., Gilpin, M., Bateson, J.H., Cheever, C., Niconovich, N.L., Pearson, S., Rittenhouse, S., Tew, D., Díez, E., Pérez, P., de la Fuente, J., Rees, M. and Rivera-Sagredo, A., Antimicrob. Agents Chemother., 46 (2002) 1880.
29. Siemann, S., Evanoff, D.P., Marrone, L., Clarke, A.J., Viswanatha, T. and Dmitrienko, G.I., Antimicrob. Agents Chemother., 46 (2002) 2450.
30. Gubernator, K. and Böhm, H.-J. (eds.) Structure-Based Ligand Design, Wiley-VCH, Weinheim, Germany, 1998 and references therein.
31. Swanstrom, R. and Erona, J., Pharmacol. Therapeut., 86 (2000) 145.
32. Schneider, G. and Böhm, H.-J., Drug Discov. Today, 7 (2002) 64.
33. Böhm, H.-J. and Stahl, M., Rev. Comput. Chem., 18 (2002) 41.
34. Carlson, H.A., Curr. Opin. Chem. Biol., 6 (2002) 447.
35. Jones, G., Willett, P., Glen, R.C., Leach, A.R. and Taylor, R., J. Mol. Biol., 267 (1997) 727.
36. Claußen, H., Buning, C., Rarey, M. and Lengauer, T., J. Mol. Biol., 308 (2001) 377.
37. Hoffmann, D., Kramer, B., Washio, T., Steinmetzer, T., Rarey, M. and Lengauer, T., J. Med. Chem. 42, (1999) 4422.
38. Charifson, P.S., Corkery, J.J., Murcko, M.A. and Walters, W.P., J. Med. Chem., 42 (1999) 5100.
39. Terp, G.E., Johansen, B.N., Christensen, I.T. and Jørgensen, F.S., J. Med. Chem., 44 (2001) 2333.
40. Stahl, M. and Rarey, M., J. Med. Chem., 44 (2001) 1035.
41. Stahl, M. and Böhm, H.-J., J. Mol. Graph. Mod., 16 (1998) 121.
42. Sybyl, Tripos Associates Inc., St. Louis, MO, USA.
43. Halgren, T.A., J. Comput. Chem., 17 (1996) 490.
44. Halgren, T.A., J. Comput. Chem., 17 (1996) 520.
45. Halgren, T.A., J. Comput. Chem., 17 (1996) 553.
46. Halgren, T.A., J. Comput. Chem., 17 (1996) 616.
47. Halgren, T.A. and Nachbar, R.B., J. Comput. Chem., 17 (1996) 587.
48. Halgren, T.A., J. Comput. Chem., 20 (1999) 720.
49. Halgren, T.A., J. Comput. Chem., 20 (1999) 730.
50. Damblon, C., Jensen, M., Papamicael, C., Barsukov, I., Ababou, A., Schofield, C.J., Olsen, L., Bauer, R. and Roberts, G.C.K., J. Biol. Chem., 278 (2003) 29240.
51. Morris, G.M., Goodsell, D.S., Halliday, R.S., Huey, R., Hart, W.E., Belew, R.K. and Olson, A.J., J. Comput. Chem., 19 (1998) 2639.
52. Hanessian, S., Moitessier, N. and Therrien, E., J. Comput.-Aided Mol. Design, 15 (2001) 873.
53. Hoops, S.C., Anderson, K.W. and Merz, K.M., J. Am. Chem. Soc., 113 (1991) 8262.
54. Dewar M.J.S. and Thiel W., J. Am. Chem. Soc., 99 (1977) 4899.
55. Dewar M.J.S. and Thiel W., J. Am. Chem. Soc., 99 (1977) 4907.
56. Rarey, M., Kramer, B., Lengauer, T. and Klebe, G., J. Mol. Biol., 261 (1996) 470.
57. Rarey, M., Wefing, S. and Lengauer, T., J. Comput.-Aided Mol. Design, 10 (1996) 41.
58. Rarey, M., Kramer, B. and Lengauer, T., J. Comput.-Aided Mol. Design, 11 (1997) 369.
59. Kramer, B., Rarey, M. and Lengauer, T., Proteins, 37 (1999) 228.
60. Goodford, P. J., J. Med. Chem., 28 (1985) 849.
61. Boobbyer, D.N.A., Goodford, P.J., McWhinnie, P.M. and Wade, R.C., J. Med. Chem., 32 (1989) 1083.
62. Wade, R.C., Clark, K.J. and Goodford, P.J., J. Med. Chem., 36 (1993) 140.
63. Wade, R.C. and Goodford, P.J., J. Med. Chem., 36 (1993) 148.
64. GRID manual, Chapter 36, cf. http://www.mol-discovery.com/docs/grid21.
65. Barone, V. and Cossi, M., J. Phys. Chem., 102 (1998) 1995.
66. Rega, N., Cossi, M. and Barone, V., J. Comput. Chem., 20 (1999) 1186.
67. Lee, C., Yang, W. and Parr, R.G., Phys. Rev. B, 37 (1988) 758.
68. Becke, A.D., J. Chem. Phys., 98 (1993) 1372.
69. Becke, A.D., J. Chem. Phys., 98 (1993) 5648.
70. Hehre, W.J., Ditchfield, R. and Pople, J.A., J. Chem. Phys., 56 (1972) 2257.
71. Ditchfield, R., Hehre, W.J. and Pople, J.A., J. Chem. Phys., 54 (1971) 724.
72. Hariharan, P.C. and Pople, J.A., Mol. Phys., 27 (1974) 209.
73. Gordon, M.S., Chem. Phys. Lett., 76 (1980) 163.
74. Hariharan, P.C. and Pople, J.A., Theor. Chim. Acta, 28 (1973) 213.
75. Stewart, J.J.P., J. Comput. Chem., 10 (1989) 209.
76. Stewart, J.J.P., J. Comput. Chem., 10 (1989) 221.
77. Frisch, M.J., Trucks, G.W., Schlegel, H.B., Scuseria, G.E., Robb, M.A., Cheeseman, J.R., Zakrzewski, V.G., Montgomery, J.A., Stratmann, R.E., Burant, J.C., Dapprich, S., Millam, J.M., Daniels, A.D., Kudin, K.N., Strain, M.C., Farkas, O., Tomasi, J., Barone, V., Cossi, M., Cammi, R., Menucci, B., Pomelli, C., Adamo, C., Clifford, S., Ochterski, J., Petersson, G.A., Ayala, P.Y., Cui, Q., Morokuma,

K., Malick, D.K., Rabuck A.D., Ragavachari, K., Foresman, J.B., Cioslowski, J., Ortiz, J.V., Stefanov, B.B., Liu, G., Liashenko, A., Piskorz, P., Komaromi, I., Gomperts, R., Martin, R.L., Fox, D.J., Keith, T., Al-Laham, M.A., Peng, C.Y., Nanayakkara, A., Gonzalez, C., Challacombe, M., Gill, P.M.W., Johnson, B.G., Chen, W., Wong, M.W., Andres, J.L., Head-Gordon, M., Replogle, E.S. and Pople, J.A., Gaussian, Inc., Pittsburg, PA, 1998.

78. Simca-P, Umetrics-AB, Umeå, Sweden.
79. Eriksson, L., Johansson, E., Kettaneh-Wold, N. and Wold, S., Multi- and Megavariate Data Analysis. Principles and Applications, Umetrics-AB, Umeå, Sweden, 2001.
80. Powell, J.W. and Whiting, M.C., Tetrahedron, 7 (1959) 305.